7. RESULTS

7.1 Effect of hMLH1 or p53 status on the mechanism of cytotoxicity of UCN-01 in colorectal cancer cell lines

7.1.1 Effect of hMLH1 status on the cellular response to UCN-01

The hMLH1 protein has been shown to contribute to the cellular mechanisms leading to G1- and G2/M-phases arrest and to induction of apoptosis [69-72]. The cytotoxic agent UCN-01 has been described to induce G1-phase arrest and apoptosis when used as a single agent [97], and to abrogate G2/M-phase arrest when used in combination with other chemotherapeutic agents [96]. We have initially observed that two human colorectal cancer cell lines differing from the presence of the *hMLH1* gene were showing a striking difference in their sensitivity to the cytotoxic agent UCN-01. In view of these observations, we have hypothesized a possible connection between hMLH1 status and the cellular response to UCN-01.

7.1.1.1 The cytotoxic effect of UCN-01 is different in hMLH1$^+$ or hMLH1$^-$ cells

In order to analyse if the presence of the hMLH1 protein had any influence on UCN-01 cytotoxicity, the nearly isogenic cell lines HCT116 (hMLH1$^-$) and HCT116+ch3 (hMLH1$^+$) were compared in MTT and clonogenic assay after treatment with UCN-01. As well, HCT116+ch2 cell line, carrying the additional chromosome 2, with no MMR-related genes, was employed as a control in the clonogenic assay.

MTT assay indicated that 2 days after start of treatment, the hMLH1$^+$ cell line was more resistant than the hMLH1$^-$ cell line (**Fig. 7A**). Six days after start of treatment the sensitivity was reversed, the hMLH1$^+$ cell line being more sensitive than the hMLH1$^-$ cell line (**Fig. 7B**). This last result was confirmed in clonogenic assay carried out 14 days after the start of treatment (**Fig. 7C**).

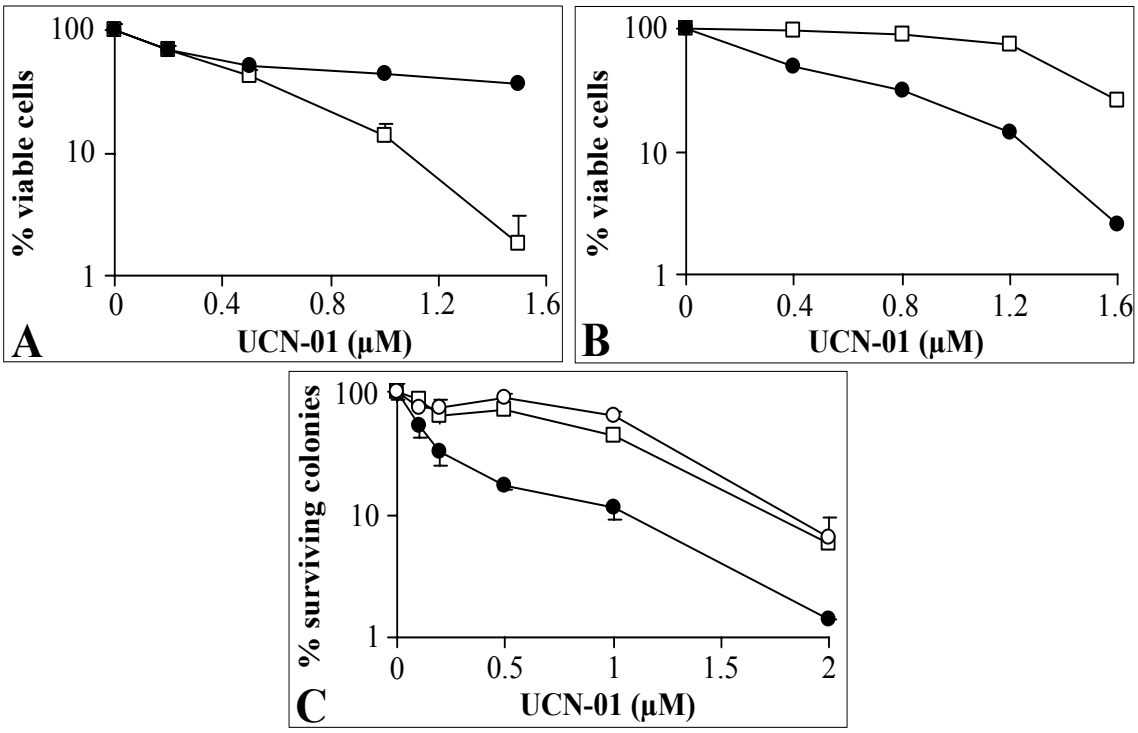

Fig. 7: Effects of hMLH1-defect on the sensitivity to UCN-01. Cells were treated 2 days with different concentrations of UCN-01. **A**: MTT assay 2 days after start of treatment. **B**: MTT assay 6 days after start of treatment. **C**: Clonogenic assay 14 days after start of treatment. HCT116+ch2 cells were employed as a control of the effect of introduction of a chromosome not carrying MMR-related genes. Results are representative of three experiments. Mean values of triplicates ± standard deviation (SD) are shown (in **A** and **B,** SD were smaller than symbols). M. Bhonde carried out experiments shown in **A** and **B**.
Symbols: —●— HCT116+ch3 (hMLH1$^+$); —□— HCT116 (hMLH1$^-$); —◇— HCT116+ch2 (hMLH1$^-$).

These results were interpreted to indicate that presence of hMLH1 exerts an influence on the susceptibility of cells to UCN-01 and that two days after start of treatment the hMLH1$^-$ cell line is more sensitive than the hMLH1$^+$ cell line to UCN-01. In the long-term assay, hMLH1$^+$ cells are more sensitive to UCN-01.

7.1.1.2 UCN-01 induces immediate apoptosis in hMLH1$^-$ cells

To test if enhanced sensitivity to UCN-01 was due to enhanced apoptosis, the concentration dependence and time course (see *7.1.1.3*) of cell death induction in hMLH1$^+$ and hMLH1$^-$ cell lines were performed.

Two days after start of treatment with 1-2 µM UCN-01, cell death was detected by trypan blue staining (**Fig. 8A**). At 2 µM UCN-01, the hMLH1$^-$ cell line was showing 80% of cell death, while the hMLH1$^+$ about 20%. The increase of subG1 fraction, as detected by FACS analysis, was also enhanced in the hMLH1$^-$ cell line (**Fig. 8B**).

Apoptosis, as measured by Cell Death Detection ELISA was enhanced 40 times in the hMLH1$^-$ cell line, while in hMLH1$^+$ cells it was 10 times higher than in the non-treated sample at the highest UCN-01 concentration tested (**Fig. 8C**).

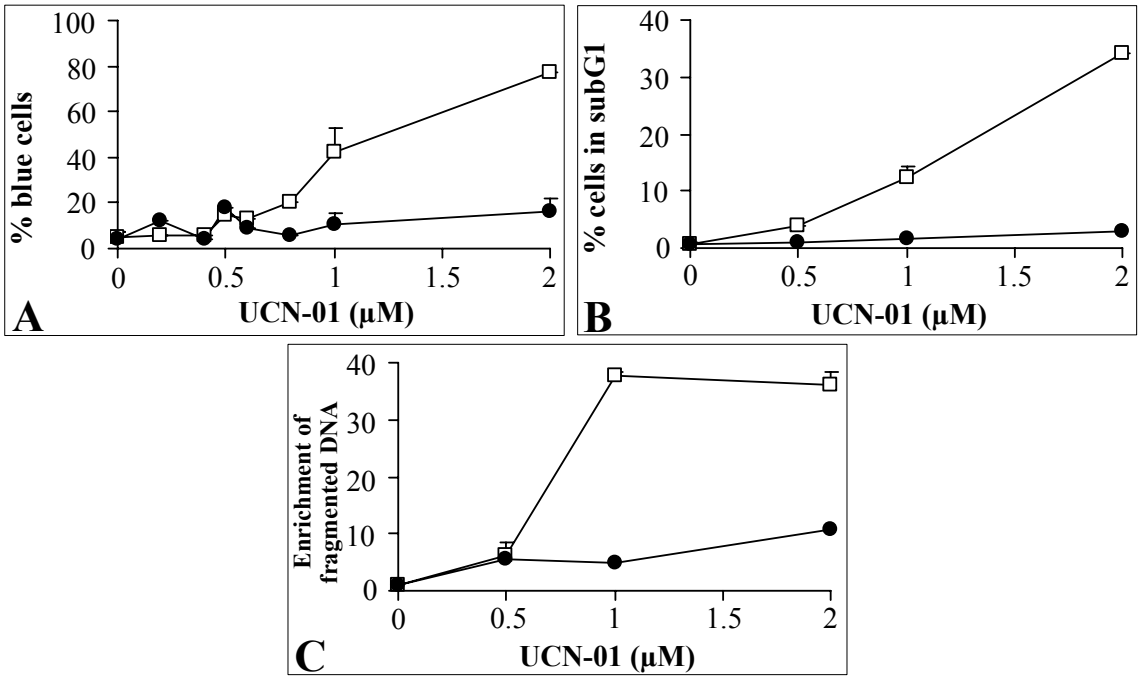

Fig. 8: hMLH1$^-$ cells are undergoing cell death after 2 days of treatment with UCN-01. Symbols are as in **Fig. 7**. **A**: Fraction of cells stained with trypan blue. **B**: Fraction of cells in subG1 as detected by FACS. **C**: Cell Death Detection ELISA. Results are representative of three experiments. Mean values of triplicates ± SD are shown.

Therefore, UCN-01 treatment induces apoptosis in the hMLH1$^-$ cell line but not in the hMLH1$^+$ cell line.

7.1.1.3 UCN-01 induces a delayed and prolonged apoptosis in hMLH1$^+$ cells

To investigate whether the strong sensitivity, observed in clonogenic assay (**Fig. 7C**), of hMLH1$^+$ cells to UCN-01 was due to a slow cell death mechanism, as observed recently in human prostate cancer cell line treated with UCN-01 [173], apoptosis was investigated in the days following treatment with UCN-01 in hMLH1$^+$ and hMLH1$^-$ cells.

To perform these and the following experiments a concentration of 1 μM UCN-01 was chosen. The time course of treatment-induced cell death demonstrated that a burst of apoptosis occurred in hMLH1$^-$ cells between 1 and 2 days from the start of treatment, showed by trypan blue staining (**Fig. 9A**), Cell Death Detection ELISA (**Fig. 9B**), subG1 fraction (**Fig. 9C**), and cleavage of PARP protein (**Fig. 9D**). At this time, hMLH1$^+$ cells were not undergoing apoptosis (**Fig. 9**). By contrast, in the hMLH1$^+$ cells apoptosis was delayed, with a maximum at 8-10 days from the start of treatment (**Fig. 9A, B, C**). PARP cleavage was not observed in hMLH1$^+$ cells even at 8-10 days from the start of treatment (**Fig. 9D**).

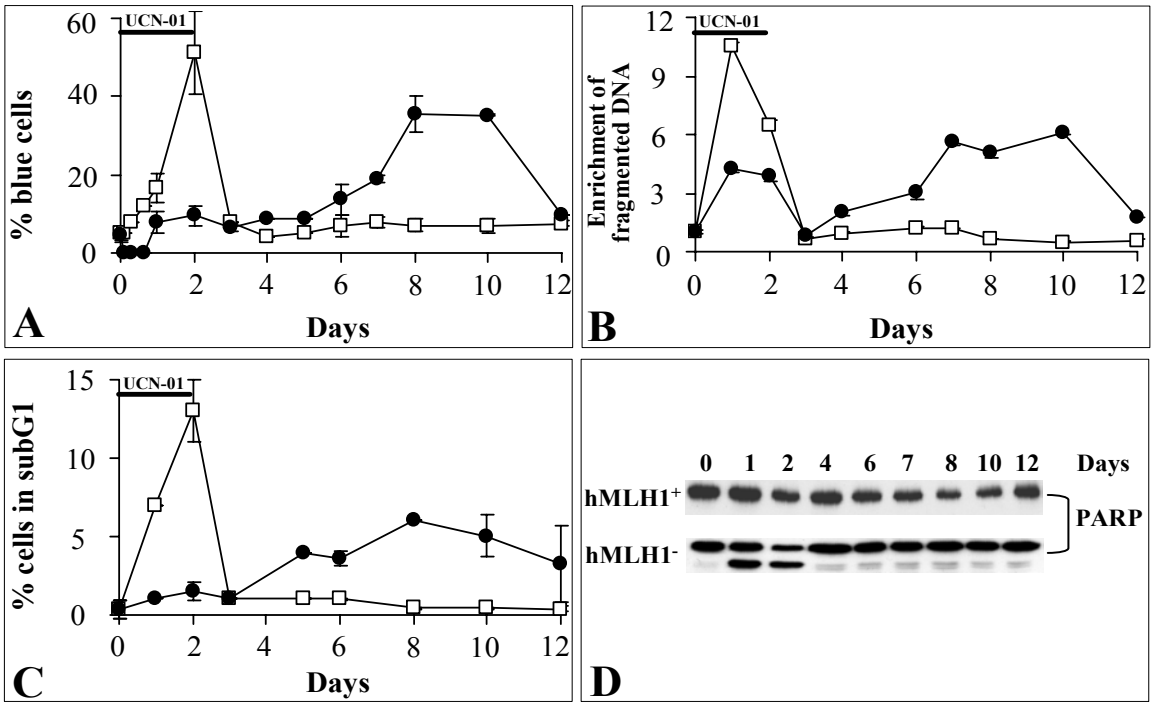

Fig. 9: Time course of cell death after treatment with 1 μM UCN-01 for 2 days. Symbols are as in **Fig. 7.** **A**: Fraction of cells stained with trypan blue. **B**: Cell Death Detection ELISA. **C**: Fraction of cells in subG1 as detected by FACS. **D**: PARP cleavage, detected in Western blot. Results are representative of three experiments. Mean values of triplicates ± SD are shown (in **B,** SD were smaller than symbols). M. Bhonde carried out the experiment shown in **D**.

These data were reinforced by morphological analysis after nuclear staining with DAPI (**Fig. 10)** and by immunocytochemistry using M30 CytoDeath monoclonal antibody, reacting with a neoepitope of cytokeratin 18 produced during apoptosis [167] (**Fig. 11**). At day 1 after start of treatment, apoptotic nuclei were not detectable in the hMLH1$^+$ cell line (**Fig. 10B**), while they were visible in the hMLH1$^-$ cell line as chromatin condensation or by the presence of apoptotic bodies (**Fig. 10E**). Eight days after start of treatment the hMLH1$^+$ cells were showing evidence of apoptosis (**Fig. 10C**) while the hMLH1$^-$ cells showed morphologically normal nuclei (**Fig. 10F**).

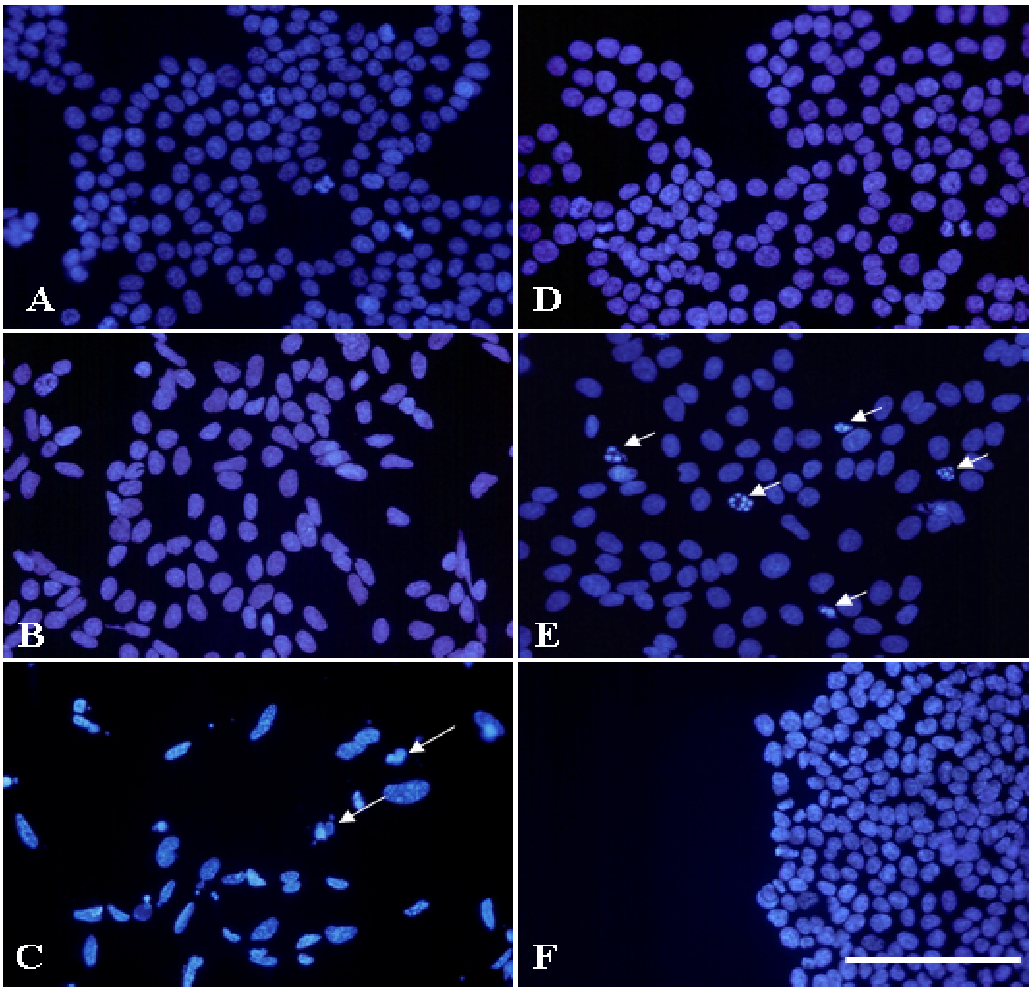

Fig. 10: DAPI staining of non-treated hMLH1$^+$ (**A**) and hMLH1$^-$ (**D**) cells or cells of the same cell lines grown for 1 day in UCN-01 (1 µM) (**B, E**) or grown for 6 days after UCN-01 treatment for 2 days (1 µM) (**C, F**). Arrows: Apoptotic nuclei. Bar: 500 µm.

By immunocytochemistry with M30 antibody no apoptotic cells were detected 1 day after start of treatment in hMLH1$^+$ cells (**Fig. 11B**), while apoptotic hMLH1$^-$ cells

expressing the cytokeratin neoepitope were visible (**Fig. 11E**). Eight days after start of treatment early apoptosis was detected in hMLH1$^+$ cells but not in hMLH1$^-$ cells (**Fig. 11C** and **11F**, respectively).

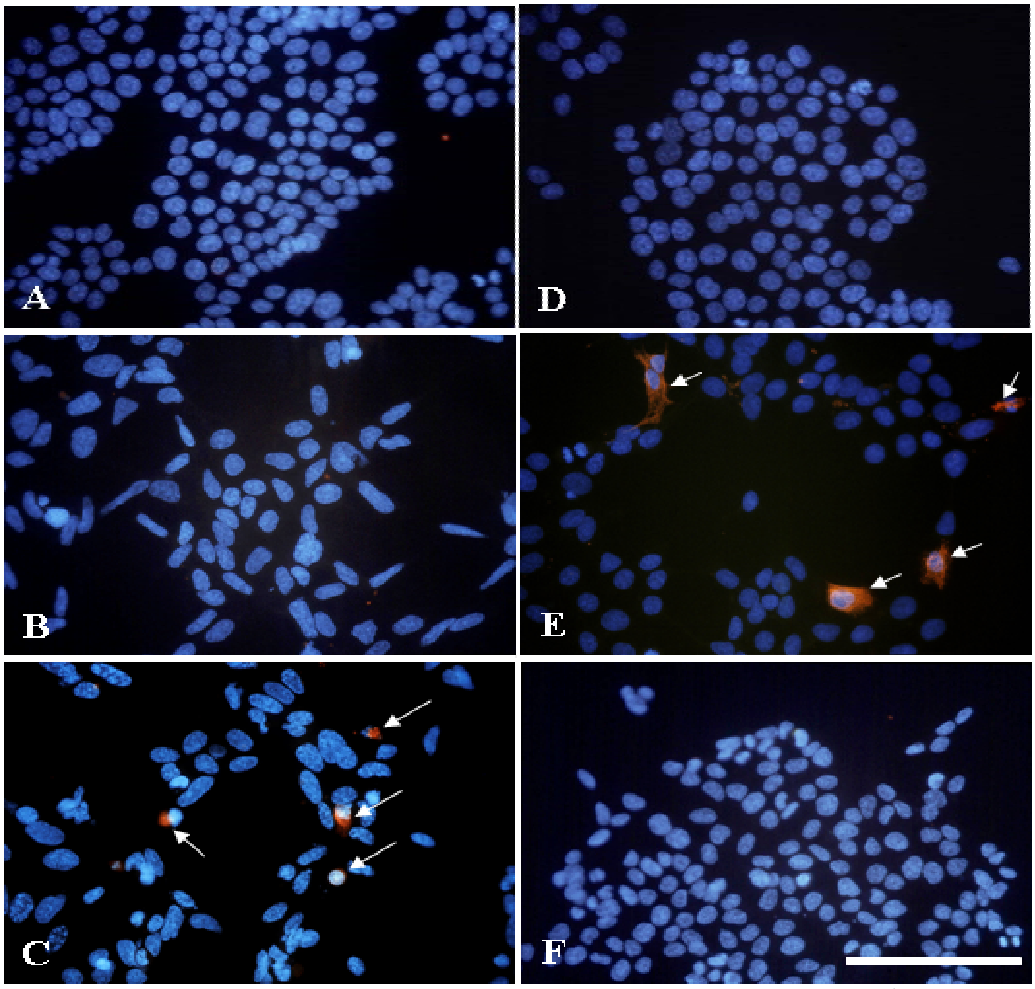

Fig. 11: Immunocytochemistry with M30 monoclonal antibody of non-treated hMLH1$^+$ (**A**) and hMLH1$^-$ (**D**) cells or cells of the same lines grown for 1 days in UCN-01 (1 µM) (**B, E**) or grown for 6 days after UCN-01 treatment for 2 days (1 µM) (**C, F**). Arrows: Early apoptotic nuclei expressing the cytokeratine 18 neoepitope. Bar: 500 µm.

Thus, in the present cell system, a functional hMLH1 protein affects the time course and the extent of UCN-01-induced apoptosis. The pathways of apoptosis were different: While the immediate reaction was PARP-mediated, the late apoptosis induction was occurring without PARP involvement.

7.1.1.4 UCN-01 induces a stronger G1-phase arrest in hMLH1$^+$ cells than in hMLH1$^-$ cells

To elucidate the process leading to the strong and immediate apoptosis observed in the hMLH1$^-$ cell line, the effects of UCN-01 on the cell cycle were investigated.

In accordance with published results obtained with cell lines originating from tumors of different tissues [97], UCN-01 induced mainly G1-phase arrest in both investigated colon carcinoma cells. The percentage of G1-phase arrested cells after treatment with different concentrations of UCN-01 was stronger in hMLH1$^+$ cells (80%-90%) than in hMLH1$^-$ cells (60%) (**Fig. 12A**). In particular, after 2 days of treatment with 1 µM UCN-01, about 2% of hMLH1$^+$ cells had a DNA content < 2N (subG1), 90% of cells had a DNA content = 2N (G1-phase) and about 7% had a DNA content = 4N (G2/M-phase) (**Fig. 12B**). hMLH1$^-$ cells showed under the same conditions 13% of cells in subG1, 70% in G1-phase and 6% of cells in G2/M-phase (**Fig. 12B**).

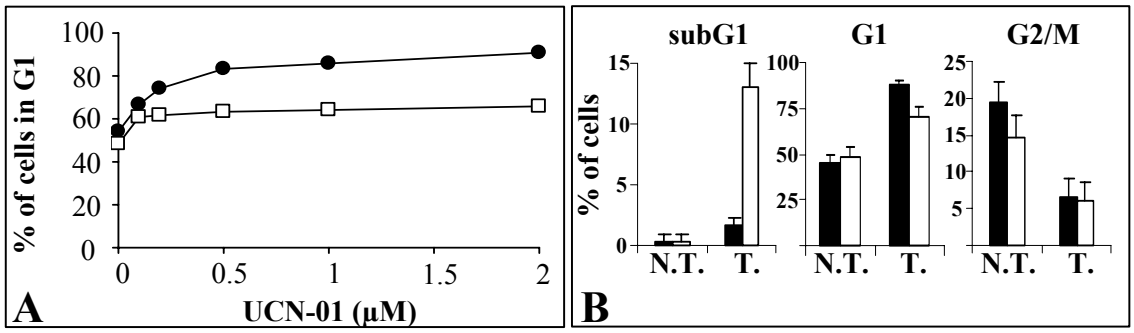

Fig. 12: UCN-01 treatment affects differently cell cycle distribution of hMLH1$^+$ or hMLH1$^-$ cells. **A**: FACS determination of the percentage of hMLH1$^+$ (—●—) and hMLH1$^-$ (—□—) cells arrested in G1-phase of the cell cycle 2 days after start of treatment with UCN-01. **B**: FACS determination of the percentage of hMLH1$^+$ (■) and hMLH1$^-$ (□) cells in subG1-, G1-, and G2/M- phases of the cell cycle in samples from cells non-treated (N.T.) and cells treated with 1 µM UCN-01 for 2 days (T.). Results are representative of three experiments. Mean values of triplicates ± SD are shown.

Thus, after UCN-01 treatment, hMLH1$^+$ cells undergo a stronger G1-phase arrest than hMLH1$^-$ cells, the difference being about 20%.

7.1.1.5 G1-phase arrest in hMLH1$^+$ cells is due to hypophosphorylation of the Rb protein and inhibition of cdk2 kinase activity

In order to understand the molecular mechanism responsible for the different extent of G1-phase arrest observed in hMLH1$^+$ ad hMLH1$^-$ cells after UCN-01 treatment, the

expression pattern of proteins whose function is related to the G1-phase of the cell cycle was analysed.

After treatment with UCN-01, p53 protein was downregulated in hMLH1$^+$ and hMLH1$^-$ cells (**Fig. 13**). p21^{CIP1} protein was downregulated already after 7 hr of UCN-01 treatment in the hMLH1$^-$ cell line, while it was found overexpressed up to 24 hr after start of treatment in the hMLH1$^+$ cell line. p21^{CIP1} levels were decreasing in both cell lines at 48 hr after start of treatment (**Fig. 13**). The expression of other proteins whose function is related to the G1-phase arrest (cdk4, cdk2 and cyclin D1), was similarly decreasing in both hMLH1$^+$ as well as in hMLH1$^-$ cell lines after 48 hr of treatment (**Fig. 13**). In addition, treatment with UCN-01 did not affect the expression levels of the hMLH1 protein, while hMSH2 protein was downregulated in hMLH1$^+$ and hMLH1$^-$ cells (**Fig. 13**).

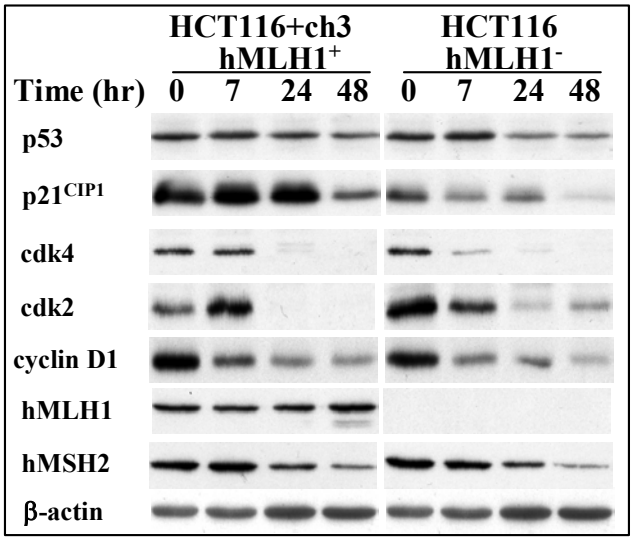

Fig. 13: Western blot analysis showing expression of the p53, p21^{CIP1}, cdk4, cdk2, cyclin D1, hMLH1, and hMSH2 proteins after treatment of hMLH1$^+$ or hMLH1$^-$ cells with UCN-01 (1 µM for 7, 24 and 48 hr). 20 µg of protein were loaded to each lane. Results are representative of at least 2 experiments. ß-actin band, detected for control of the loaded protein amount, was the same in all lanes.

Rb protein is a major regulator of the G1-phase arrest. When Rb is hyper-phosphorylated, it is unable to bind and inactivate the transcription factor E2F1, leading to transactivation of E2F1-dependent genes and progression to S-phase [22]. Thus, the hypophosphorylated form of Rb is associated with G1-phase arrest, while the hyperphosphorylated form of Rb indicate an active cell cycle status of the cells. When cells were treated with different concentrations of UCN-01 for 1 day, hypophosphorylated forms of Rb protein (Rb-P) in hMHL1$^+$ cells were already present at 0.1 µM UCN-01 (**Fig. 14A**). At higher UCN-01 concentrations, the Rb protein was

present in these cells only in its hypophosphorylated state. In hMLH1$^-$ cells the Rb protein was maintained up to 0.5 μM UCN-01 in both forms, hyper- as well as hypo-phosphorylated (Rb-PP and Rb-P) (**Fig. 14A**). Similarly, a time course up to 2 days of treatment with UCN-01 at 1 μM, showed the prevalence of the hypophosphorylated form of Rb in hMLH1$^+$ cells, while in hMLH1$^-$ cells the protein was maintained in its multiple phosphorylated forms, prevalently in the hyperphosphorylated form (**Fig. 14B**).

Liberation of E2F1 leads to transcriptional activation of the *cyclin E* gene. The cyclin E protein forms a complex with cdk2; cdk2/cyclin E activity phosphorylates further Rb leading to its complete activation. Possibly, cdk2/cyclin E kinase was differently activated in hMLH1$^+$ or hMLH1$^-$ cells after UCN-01 treatment; this could explain the different Rb-phosphorylation observed in these cell lines. To test this hypothesis, cdk2 was immunoprecipitated. The immunoprecipitates were analysed in Western blot for the presence of the cdk2 protein: cdk2 amount was decreasing to the same extent in the immunoprecipitates from the two cell lines after treatment with UCN-01 (**Fig. 14C**, immunoprecipitates). The downregulation of cdk2 protein after treatment with UCN-01 was also observed by Western blot in lysates (**Fig. 13** and **Fig. 14C**, lysates). One of the mechanisms of regulation of the activity of cdk2/cyclin E kinase is binding of either p21^{CIP1} or p27^{KIP1} proteins to cdk2/cyclin E. The down-regulation of p21^{CIP1} to a similar extent in hMLH1$^+$ and hMLH1$^-$ cell lines (**Fig. 13**) suggested that this protein was not involved in inhibition of cdk2/cyclin E activity. p27^{KIP1} was overexpressed to approximately the same extent in hMLH1$^+$ and hMLH1$^-$ cells after UCN-01 treatment (**Fig. 14C,** lysates). However, after immunoprecipitation of cdk2, p27^{KIP1} was detected in Western blot only in the immunoprecipitates from hMLH1$^+$ cells after treatment with UCN-01 (**Fig. 14C**, immunoprecipitates). p27^{KIP1} was barely detectable in immunoprecipitates of hMLH1$^-$ cells (**Fig. 14C**, immunoprecipitates). Concomitantly, cdk2 kinase activity, measured by phosphorylation of histone H1, was inhibited to 30% in hMLH1$^+$ cells, while it was inhibited to a lesser extent (67%) in hMLH1$^-$ cells (**Fig. 14C**).

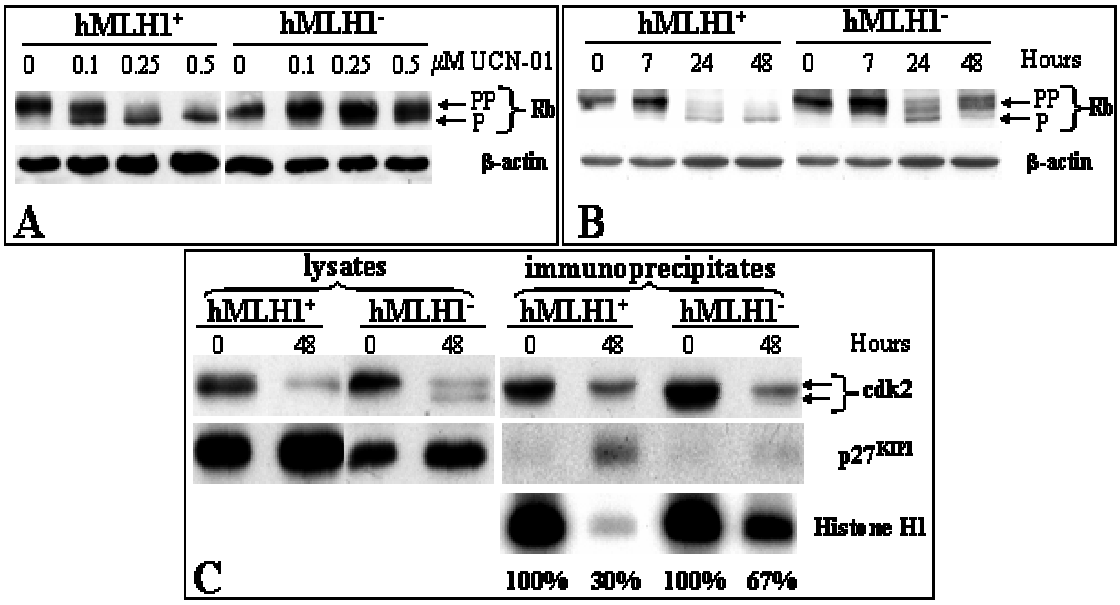

Fig. 14: **A** and **B**: UCN-01 treatment affects the phosphorylation status of the Rb protein in hMLH1$^+$ cells but less in hMLH1$^-$ cells. Western blot of lysates, detected with antibody against Rb protein. 25 µg of lysates were applied to each lane. ß-actin band, detected for control of the loaded protein amount, was the same in all lanes. **A**: Extent of Rb phosphorylation at different concentration of UCN-01, treatment for 1 day. **B**: Extent of Rb phosphorylation at different hours after start of treatment with 1 µM UCN-01.Rb-P indicates hypophosphorylated Rb protein, while Rb-PP indicates hyperphosphorylated Rb protein. **C**: Lysates (left) and immunoprecipitates (right) from hMLH1$^+$ and hMLH1$^-$ cells non-treated or treated for 2 days with 1 µM UCN-01, were analysed for the presence of cdk2 and p27^{KIP1} proteins by Western blot. Precipitations were carried out with the anti-cdk2 antibody. cdk2 kinase activity, measured as histone H1 phosphorylation, was visualised by autoradiography. U. Kobalz performed experiment shown in **A**, M.-L. Hanski performed experiments shown in **B** and **C**.

The present data show that the magnitude of G1-phase arrest induced by UCN-01 correlates with the extent of hypophosphorylation of the Rb protein as well as with the inhibition of the activity of the cdk2 kinase.

Thus, the major effect of UCN-01 on cell cycle is the induction of an accumulation of cells in G1-phase, and this effect is stronger in hMLH1$^+$ than in hMLH1$^-$ cells. In hMLH1$^+$ cells, the stronger G1-phase arrest is associated with hypophosphorylation of the Rb protein and inactivation of the cdk2 kinase activity. Inactivation of cdk2 activity in hMLH1$^+$ cells was correlated with inhibitory binding of the p27^{KIP1} protein to the kinase complex.

7.1.1.6 hMLH1$^-$ cells partly escape from G1-phase arrest induced by UCN-01

The incomplete G1-phase arrest characterizing the hMLH1$^-$ cell line suggested that some of these cells were entering cell cycle after UCN-01 treatment.

In order to estimate the percentage of cells able to escape the G1-phase arrest, cells were treated with 1 μM UCN-01 for 24 hr and then cell escaping from the G1-phase were trapped in G2/M-phase by treatment with nocodazole for additional 17 hr.

Under these conditions, about 90% of hMLH1$^+$ and 60% of hMLH1$^-$ cells were arrested in G1-phase after UCN-01 treatment, as measured by FACS (**Fig. 15A**). When nocodazole was added, the percentage of hMLH1$^+$ cells arrested in G1-phase was not altered, while there was a drop of 10% in the percentage of hMLH1$^-$ cells arrested in G1-phase (from 60% to 50% after UCN-01 without or with nocodazole, respectively) (**Fig. 15A**, upper panel). Concomitantly, there was an increase of 10% in the percentage of hMLH1$^-$ cells arrested in G2/M-phase, from 4 to 15% after UCN-01 without or with nocodazole, respectively (**Fig. 15A**, lower panel). By contrast, the addition of nocodazole to UCN-01 did not change the percentage of hMLH1$^+$ cells arrested in G2/M-phase (**Fig. 15A**, lower panel). Nocodazole used as a single agent induced a strong G2/M-phase arrest (90%) in both hMLH1$^+$ and hMLH1$^-$ cells (data not shown).

These findings were confirmed by determination of the percentage of mitotic nuclei of hMLH1$^+$ or hMLH1$^-$ cells after treatment with UCN-01 and nocodazole. hMLH1$^-$ cells showed an increase of 5% in mitotic cells between cells treated only with UCN-01 (1% mitotic nuclei) or cells treated with UCN-01 and nocodazole (6% mitotic nuclei) (**Fig. 15B**). On the other hand, the percentage of mitotic cells was not affected in hMLH1$^+$ cells after addition of nocodazole to UCN-01 (**Fig. 15B**).

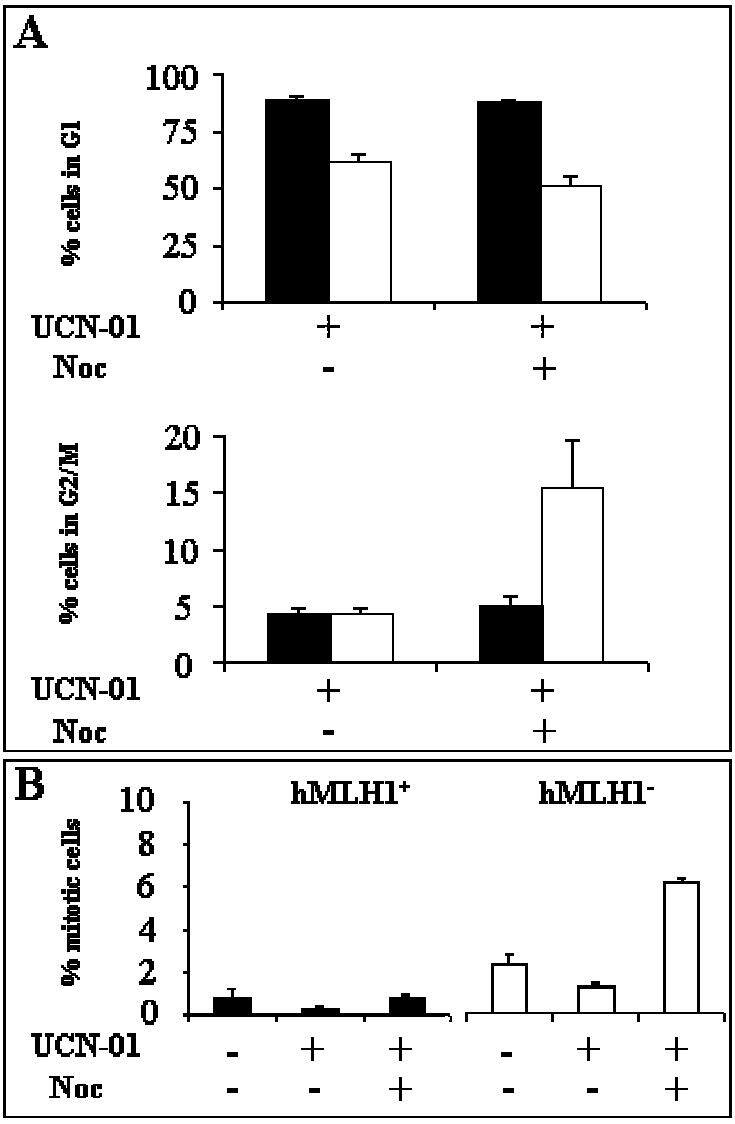

Fig. 15: hMLH1$^-$ cells (□), but not hMLH1$^+$ cells (■), partly escape from the G1-phase arrest induced by UCN-01. **A:** FACS analysis of hMLH1$^+$ or hMLH1$^-$ cells treated with UCN-01 and nocodazole. **Upper panel**: Percentage of cells in G1-phase. **Lower panel**: Percentage of cells in G2/M-phase. **B**: Percentage of mitotic cells, evaluated after staining with DAPI, in hMLH1$^+$ and hMLH1$^-$ cells treated with UCN-01 and nocodazole. Treatment conditions were: nocodazole alone (17 hr, 166 nM), UCN-01 alone (41 hr, 1 μM), or UCN-01 + nocodazole (24 hr UCN-01 1 μM, then nocodazole was added in the presence of UCN-01 for the successive 17 hr at a final concentration of 166 nM). Mean values of three independent experiments ± SD are shown.

Thus, after UCN-01 treatment hMLH1$^+$ cells are completely arrested in G1-phase, while a small percentage of hMLH1$^-$ cells undergo another mitotic cycle.

7.1.1.7 hMLH1$^-$cells, but not hMLH1$^+$ cells, entering the cell cycle, undergo apoptosis

The data obtained hitherto lead to the question why hMLH1$^-$ cell line treated with UCN-01 carries out immediate apoptosis while the hMLH1$^+$ cell line does not.

It has been shown in S-phase-arrested myeloblastic cells that UCN-01 was able to initiate an apoptotic cascade [174]. To test if S-phase was sensitizing also colon carcinoma cells to UCN-01, cells were blocked in S-phase by pretreatment with

aphidicolin. After 1 day, about 40% of hMLH1$^+$ cells and 60% of hMLH1$^-$ cells were accumulated in S-phase. At this time, UCN-01 was added for the successive day in the presence of aphidicolin; while hMLH1$^+$ cells substantially remained arrested in S-phase, the percentage of hMLH1$^-$ cells arrested in S-phase diminished from 60% to about 20% and, at the same time, the percentage of cells in subG1 increased from 10% with UCN-01 alone to 33% with UCN-01 + aphidicolin (**Fig. 16**). Preincubation with aphidicolin for 2 days caused hMLH1$^+$ and hMLH1$^-$ cells to arrest mainly in G2/M-phase. Under these conditions, treatment with UCN-01 for the successive day also induced a strong enhancement of apoptosis in hMLH1$^-$ but not in hMLH1$^+$ cells (**Fig. 16**).

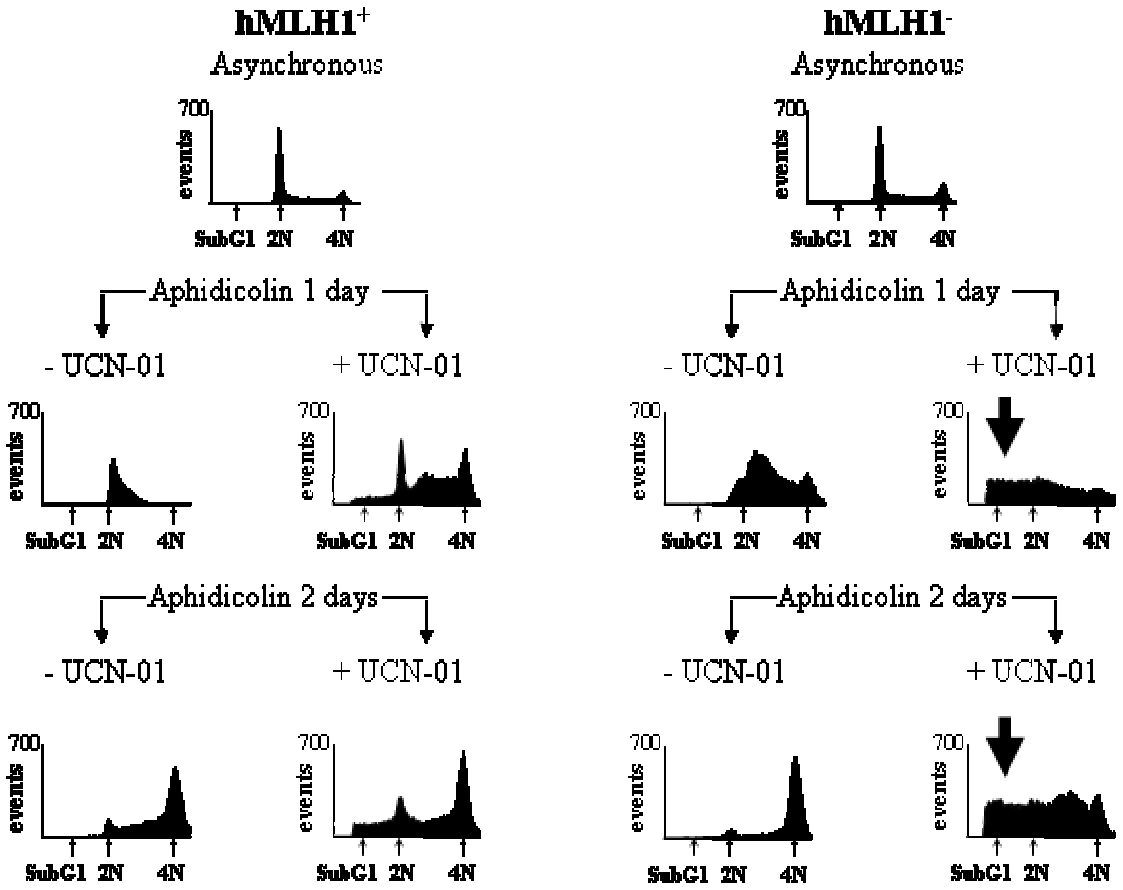

Fig. 16: UCN-01 commits to apoptosis hMLH1$^-$ cells arrested in S- or G2/M- phase of the cell cycle. Representative FACS diagrams for each non-treated and non-synchronized cell line, *versus* synchronized for 1 or 2 days with 1 μM aphidicolin in S- and G2/M- phases, respectively. Addition of UCN-01 after synchronization causes an increase of the subG1 population in hMLH1$^-$ cells (thick arrow), but not in hMLH1$^+$ cells. Results are representative of two independent experiments.

The finding that hMLH1$^-$ cells arrested in G2/M-phase undergo massive apoptosis after UCN-01 treatment while hMLH1$^+$ cells do not, was reinforced using two specific inhibitors of mitotic progression, nocodazole and colcemid. After 3 hr of nocodazole treatment, hMLH1$^+$ and hMLH1$^-$ cells were arrested to about 60% in G2/M-phase. After 24 hr of colcemid treatment, hMLH1$^+$ and hMLH1$^-$ cells were arrested to 90% in G2/M-phase. UCN-01 was added at this time points for the successive 24 hr. hMLH1$^+$ cells remained arrested in G2/M-phase when UCN-01 was incubated with nocodazole or with colcemid. In hMLH1$^-$ cells, apoptosis was strongly enhanced when cells were treated with combinations of UCN-01 and nocodazole or of UCN-01 and colcemid; after either treatment, the percentage of cells in subG1 peak (**Fig. 17A**) and the PARP cleavage were increased (**Fig. 17B**).

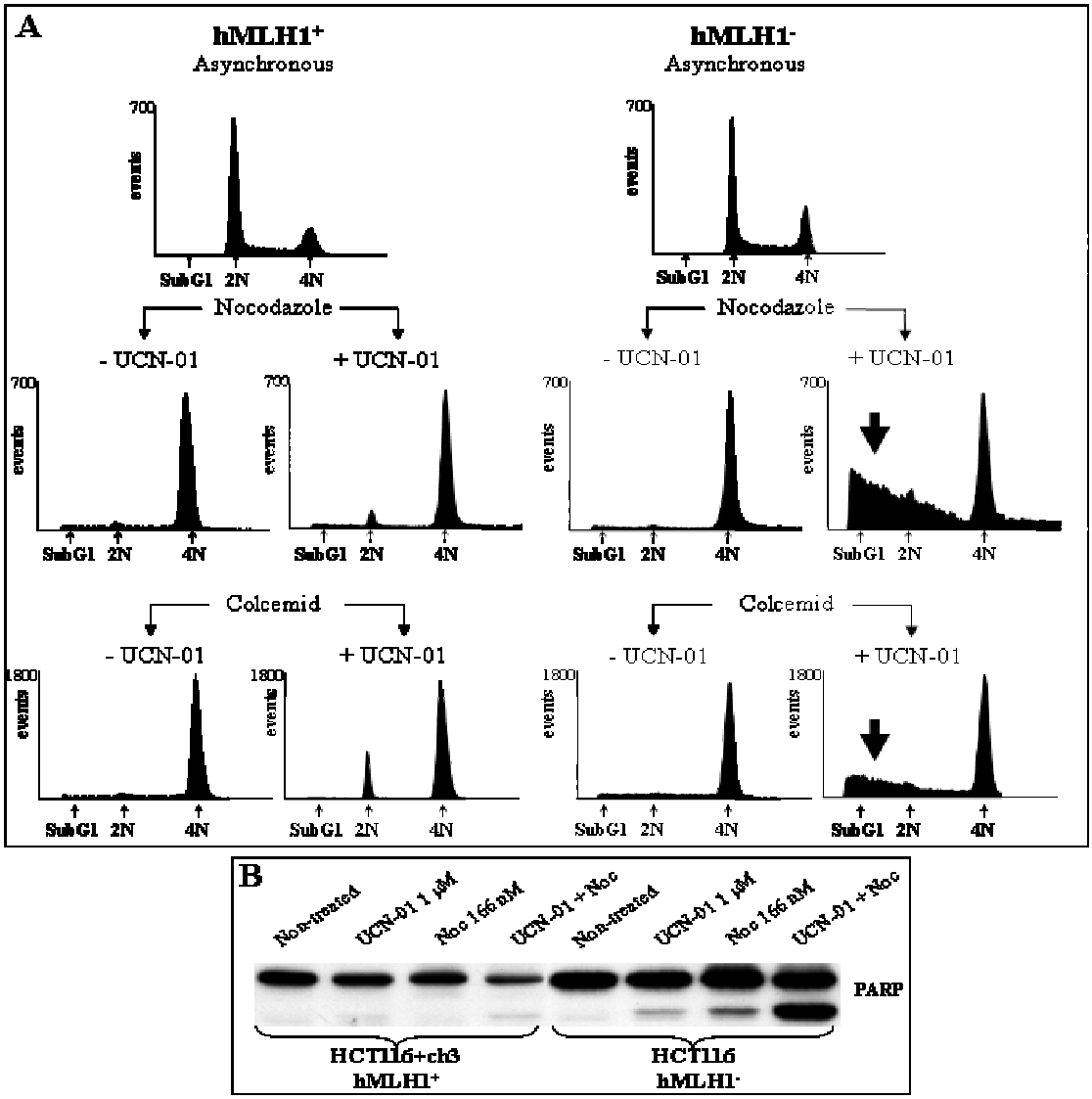

Fig. 17: UCN-01 commits to apoptosis hMLH1$^-$ cells arrested in mitotic-phase of the cell cycle. **A**: Representative FACS diagrams for each non-treated and non-synchronized cell line, *versus* synchronized in G2/M-phase obtained by treatment for 3 hr with 166 nM nocodazole or for 24 hr with 54 nM colcemid. Addition of UCN-01 after synchronization causes a strong increased of the subG1 population in hMLH1$^-$ cells (thick arrow), but not in hMLH1$^+$ cells. **B**: PARP cleavage, detected in Western blot, is strongly enhanced in hMLH1$^-$ cells after treatment with a combination of UCN-01 + nocodazole. Results are representative of two to four independent experiments.

Thus, after UCN-01 treatment hMLH1$^+$ cells are completely and permanently arrested in G1-phase, while a percentage of hMLH1$^-$ cells undergo another mitotic cycle. Progression through DNA replication and mitosis makes these cells vulnerable to UCN-01 cytotoxicity.

7.1.1.8 Apoptosis induced by UCN-01 is not correlated to changes of expression of Bax and Bcl-2 proteins

In order to elucidate the mechanism of the different apoptotic reaction observed in hMLH1$^+$ and hMLH1$^-$ cells to UCN-01, the expression levels of two members of the Bcl-2 family of proteins were analysed in a time-course experiment by means of Western blot (**Fig. 18**). The protein levels of Bax and Bcl-2 did not significantly change after 2 days of treatment.

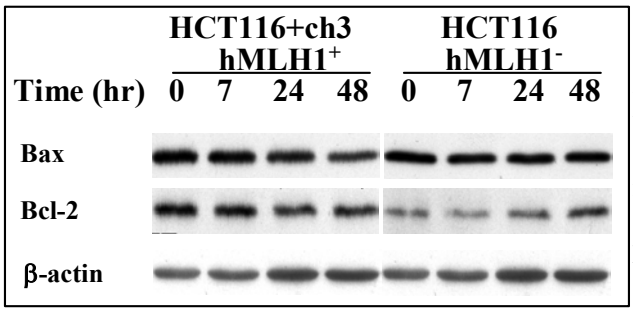

Fig. 18: Western blot analysis showing expression of the Bax and Bcl-2 proteins after treatment of hMLH1$^+$ or hMLH1$^-$ cells with UCN-01 (1 µM for 7, 24 and 48 hr). 20 µg of protein were loaded to each lane. Results are representative of at least 2 experiments. ß-actin band, detected for control of the loaded protein amount, was the same in all lanes.

Thus, expression levels of Bax and Bcl-2 proteins are not affected by UCN-01 treatment.

7.1.1.9 UCN-01 is inducing MEK2 upregulation in hMLH1$^+$ cell line at the mRNA level

In order to detect genes whose expression was differentially regulated after UCN-01 treatment in hMLH1$^+$ *versus* hMLH1$^-$ cells, differential hybridization (Atlas™ Human Cell Cycle cDNA Expression Array) was performed. It was found that the expression of the *mitogen-activated protein kinase kinase 2* gene (*MAP kinase kinase 2*, *MAPKK2*, *MEK2* gene) was 2.5 fold upregulated in hMLH1$^+$ treated cells in comparison to hMLH1$^-$ treated cells (data not shown). This finding was confirmed in RT-PCR (**Fig. 19**).

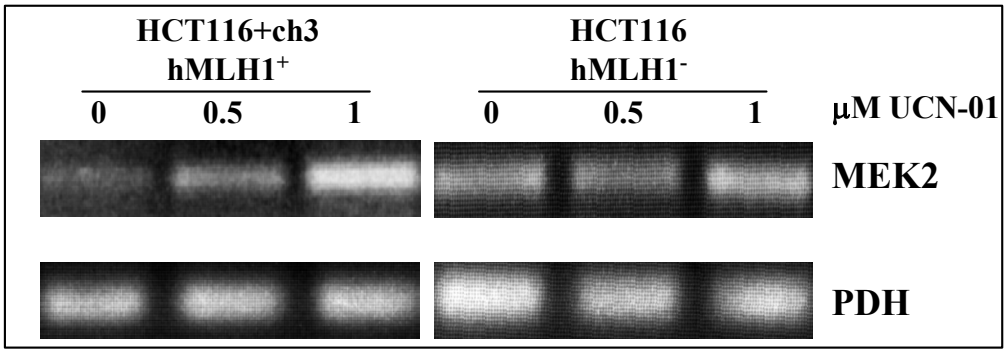

Fig. 19: MEK2 mRNA expression in hMLH1$^+$ or hMLH1$^-$ cells after UCN-01 treatment (0.5 µM and 1 µM for 2 days), determined by RT-PCR. Results are representative of two experiments. Pyruvate dehydrogenase (PDH) RT-PCR detected for control of amplified cDNA was the same in all lanes. RT-PCR was carried out by Dr. E. Riede and by D. Moorthy. RT-PCR conditions are described in Material and Methods.

7.1.1.9.1 Inhibition of MEK1/2 kinase activities enhances UCN-01-induced short-term apoptosis in hMLH1$^-$ cells

To check a possible involvement of the MAP kinase pathway in response to UCN-01 treatment, MEK1/2 activities were evaluated in Western blot by analysing the phosphorylation of ERK1/2, the only known target proteins of the MEK1/2 kinases [175]. A similar ERK1/2 phosphorylation (ERK-P) by UCN-01 was observed in hMLH1$^+$ and in hMLH1$^-$ cells: It reached a maximum after 48 hr of exposition to UCN-01 (**Fig. 20**).

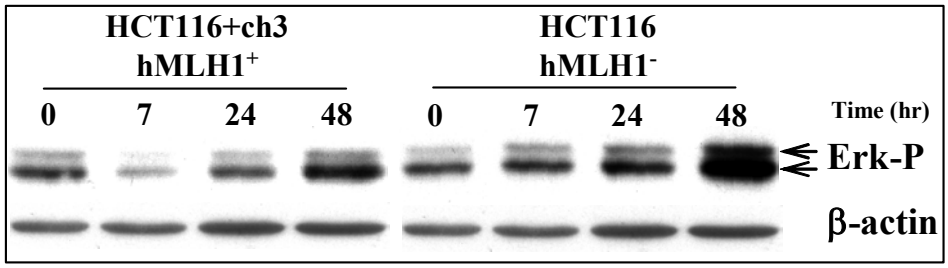

Fig. 20: Western blot analysis showing expression of the phosphorylated ERK1/2 (ERK-P) proteins after treatment of hMLH1$^+$ or hMLH1$^-$ cells with UCN-01 (1 µM for 7, 24 and 48 hr). 20 µg of protein were loaded to each lane. Results are representative of at least 4 experiments.

Inhibition of MEK1/2 kinases by two specific inhibitors, PD98059 and U0126, did not induce apoptosis in HCT116 cell lines (**Fig. 21**). However, treatment of hMLH1$^+$ or

hMLH1$^-$ cells with UCN-01 in combination with either of the two inhibitors caused a strong enhancement of apoptosis in hMLH1$^-$ cells, detectable by trypan blue staining and by PARP cleavage in Western blot. By contrast, hMLH1$^+$ cells did not undergo apoptosis under these conditions (**Fig. 21**).

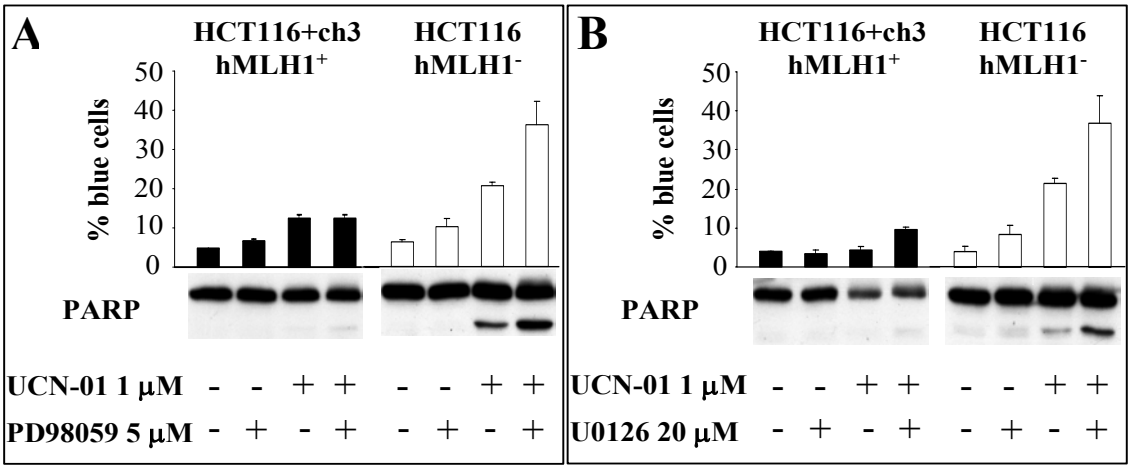

Fig. 21: Inhibition of MEK1/2 by PD98059 or U0126 enhances UCN-01-induced apoptosis in hMLH1$^-$ cells but not in hMLH1$^+$ cells. Cells were pretreated for 30 min with 5 µM PD98059 (**A**) or with 20 µM U0126 (**B**) before addition of 1 µM UCN-01 for the successive 24 hr. Results of trypan blue staining and PARP cleavage are shown as readout of cell death and apoptosis. Mean values of four independent experiments ± SD are shown.

Analysis of cell cycle after inhibition of MEK1/2 by U0126 showed that cells arrested prevalently in G1-phase (**Fig. 22**). When HCT116 cells were preincubated with U0126 for 30 min and then UCN-01 was added for the successive 24 hr, hMLH1$^+$ cells remained arrested in G1-phase (80%), while a part of hMLH1$^-$ cells left the G1-phase arrest (from 80% to 60% after treatment with U0126 without or with UCN-01, respectively) and appeared in the subG1 peak (30%) (**Fig. 22**).

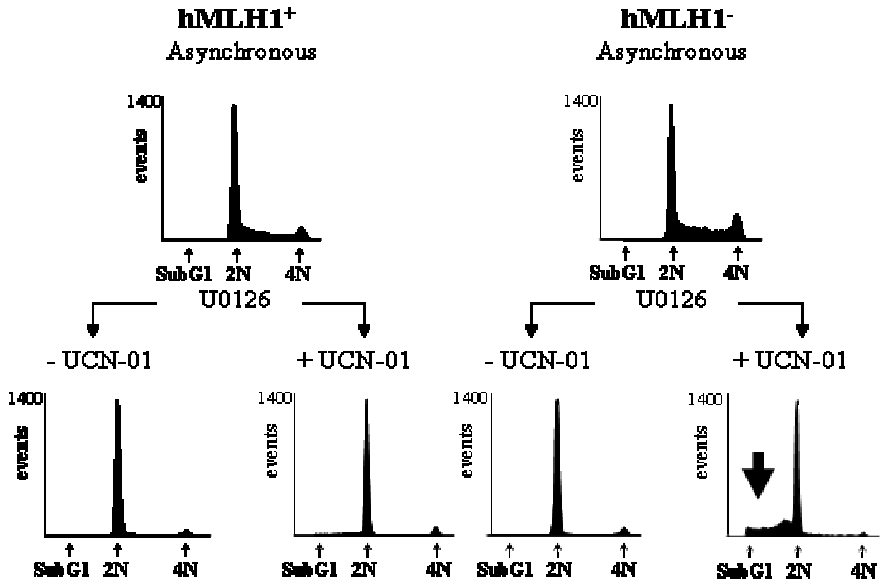

Fig. 22: UCN-01 in combination with U0126, an inhibitor of MEK1/2 kinases, enhances apoptosis in hMLH1$^-$ cells (thick arrow), and this effect is accompanied by a less extensive G1-phase arrest. hMLH1$^+$ cells remain strongly arrested in G1-phase and do not undergo apoptosis. FACS diagrams of non-treated cells, *versus* cells treated with U0126 (24.5 hr, 20 μM) or with U0126 (24.5 hr, 20 μM) + UCN-01(24 hr, 1 μM). Results are representative of two experiments.

Thus, UCN-01-induced apoptosis in hMLH1$^-$ cells is enhanced by inhibition of MEK1/2 activities. Enhancement of apoptosis is accompanied by reduction of the number of cells arrested in the G1-phase of the cell cycle.

It can be concluded from the data hitherto presented, that the absence of the hMLH1 protein affects the cellular response to UCN-01. hMLH1$^-$ cells could not maintain a tight G1-phase arrest due to less binding of the $p27^{KIP1}$ protein to cdk2 kinase and to maintenance of cdk2 kinase activity. These cells entered the cell cycle and were targeted to apoptosis when passing through S- and G2/M-phases. Inhibition of MEK1/2 kinases caused hMLH1$^-$ cells to escape partially from the G1-phase arrest induced by UCN-01, and, analogously, committed them to apoptosis. On the contrary, hMLH1$^+$ cells underwent a tight G1-phase arrest after UCN-01 treatment that prevented them to undergo apoptosis. In the following days after treatment, hMLH1$^+$ cells underwent a slow cell death not mediated by caspase activation, and were more sensitive than hMLH1$^-$ cells to UCN-01 as measured in clonogenic assay.

7.1.2 Effect of p53 status on the cellular response to UCN-01

We observed that two human colorectal cancer cell lines differing in the presence of the *p53* gene were showing a difference in sensitivity to UCN-01. Since the p53 tumor-suppressor protein has been shown to contribute to the cellular mechanism leading to apoptosis, and since the agent UCN-01 has been described to induce apoptosis, we have hypothesized a possible connection between p53 status and susceptibility to UCN-01.

7.1.2.1 $p53^{-/-}$ cells are less susceptible to UCN-01 than $p53^{+/+}$ cells

In order to analyse if the p53 status had any influence on UCN-01 cytotoxicity, the two isogenic cell lines HCT116 ($p53^{+/+}$,$hMLH1^{-}$) and HCT116 $p53^{-/-}$ ($p53^{-/-}$,$hMLH1^{-}$), thereafter named as $p53^{+/+}$ and $p53^{-/-}$, were compared in clonogenic assay, carried out 14 days after the start of treatment with UCN-01. It was found that the $p53^{-/-}$ cell line was more resistant than the $p53^{+/+}$ cell line (**Fig. 23**).

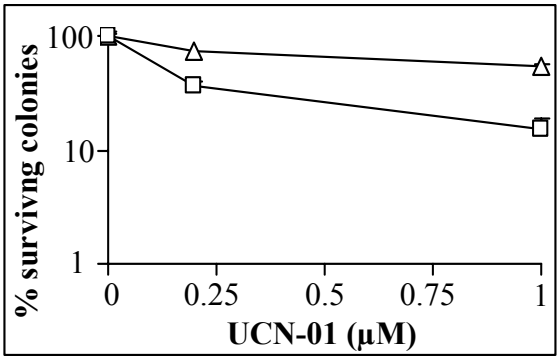

Fig. 23: Effect of *p53* gene loss on the sensitivity to UCN-01 shown in clonogenic assay after 14 days from the start of treatment. Results are representative of three independent experiments. Mean values of triplicates ± SD are shown.
Symbols: —□— HCT116 ($p53^{+/+}$); —△— HCT116 ($p53^{-/-}$).

This result indicates that the p53 status exerts an influence on the susceptibility of cells to UCN-01 and that in the long-term assay the sensitivity to UCN-01 is higher in the $p53^{+/+}$ cell line.

7.1.2.2 UCN-01 induces apoptosis in $p53^{+/+}$ but not in $p53^{-/-}$ cells

In order to clarify if the sensitivity of the $p53^{+/+}$ cell line is associated with apoptosis induction after UCN-01 treatment, the dependence of cell death induction on UCN-01 treatment was analysed in HCT116 $p53^{+/+}$ or $p53^{-/-}$ cell lines.

Two days after start of treatment with 0.2-2 μM UCN-01, cell death was detected by trypan blue staining (**Fig. 24A**). At 2 μM, the $p53^{+/+}$ cell line was showing 70% of cell death, while $p53^{-/-}$ cells about 20%. The subG1 fraction of cells, detected by FACS analysis, was also increasing in $p53^{+/+}$ cells up to 20% at 1 μM UCN-01, while it remained as in the non-treated sample in $p53^{-/-}$ cells (**Fig. 24B**). Fragmented DNA, measured by Cell Death Detection ELISA, was enriched of 16 times with respect to the non-treated sample in $p53^{+/+}$ cells, while the enrichment was only 2 times higher than in the non-treated $p53^{-/-}$ cells at 1 μM UCN-01 (**Fig. 24C**).

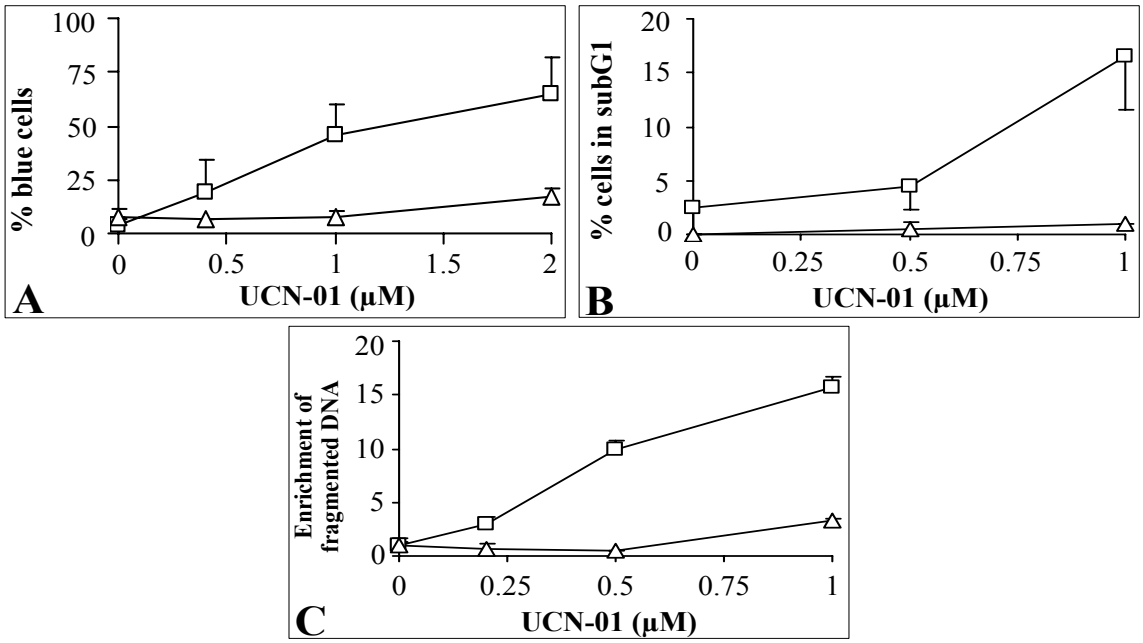

Fig. 24: Cell death is induced in $p53^{+/+}$ but not in $p53^{-/-}$ cells after 2 days treatment with UCN-01. Symbols are as in **Fig. 23**. **A**: Fraction of cells stained with trypan blue. **B**: Fraction of cells in subG1 as detected by FACS. **C**: Cell Death Detection ELISA. Results are representative of two experiments. Mean values of triplicates ± SD are shown.

Thus, the greater sensitivity of $p53^{+/+}$ cells to UCN-01 observed in clonogenic assay (**Fig. 23**) correlated to induction of apoptosis in this cell line (**Fig. 24**), while in the $p53^{-/-}$ cell line no apoptosis was detected; therefore, these cells were resistant to UCN-01.

In conclusion, the p53 protein appears to be a determinant of the apoptotic response induced by UCN-01 in the human colorectal cell line system used.

7.2 Effect of p53 or hMLH1 status on the mechanism of cytotoxicity of CPT-11 in colorectal cancer cell lines

We wished to investigate the effects of lesions in the *p53* gene and in the hMLH1 molecule on the mechanism of action and on the cytotoxicity of CPT-11 towards colon carcinoma cells *in vitro*. For this purpose, we systematically compared the results of different methods, obtained in three cell lines differing in the p53 and/or hMLH1 status.

7.2.1 p53 loss or hMLH1 defect affect sensitivity to CPT-11 measured in MTT assay but not in clonogenic assay

In order to analyse if the p53- or the hMLH1- status had any influence on CPT-11 cytotoxicity, the nearly isogenic cell lines HCT116 ($p53^{+/+}$,$hMLH1^{-}$), HCT116+ch3 ($p53^{+/+}$,$hMLH1^{+}$), and HCT116 $p53^{-/-}$ ($p53^{-/-}$,$hMLH1^{-}$) were compared in MTT and in clonogenic assays. The MTT assay, carried out five days after start of treatment with CPT-11, showed that the $p53^{+/+}$,$hMLH1^{+}$ cell line was the most resistant one, followed by the $p53^{+/+}$,$hMLH1^{-}$ cell line which showed an intermediate susceptibility, whereas the $p53^{-/-}$ cell line was the most sensitive one (**Fig. 25A**). These differences were not due to the different conversion of CPT-11 to its active form SN-38, since the specific activity of carboxylesterase was similar in the homogenates of the three cell lines (measurements carried out in our laboratory by M. Bhonde). The observed difference in cytotoxicity towards $p53^{+/+}$ and $p53^{-/-}$ cells corresponds to the previously obtained results with camptothecin, of which CPT-11 is a hydroxylated derivative, and whose cytotoxicity is also dependent on the p53 status of the cells [146].

By contrast to the MTT result, in the clonogenic survival assay neither p53 nor hMLH1 lesions appeared to affect the cytotoxicity to CPT-11 (**Fig. 25B**), as reported previously [144, 145]. The cellular reactions underlying these divergent results were therefore investigated.

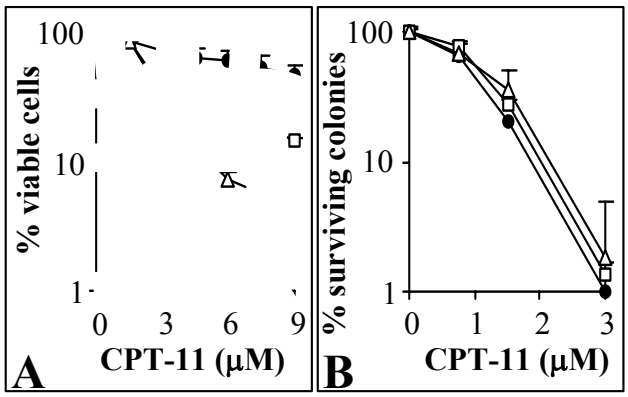

Fig. 25: Effects of *p53* mutation or hMLH1 defect on the sensitivity to CPT-11. Cells were treated 2 days with different concentrations of CPT-11. **A**: MTT assay 5 days after start of treatment. **B**: Clonogenic assay 14 days after start of treatment. Results are representative of three experiments. Mean values of triplicates ± SD are shown. Experiment shown in **A** was carried out by M. Bhonde.
Symbols: HCT116+ch3 ($p53^{+/+}$,$hMLH1^{+}$); HCT116 ($p53^{+/+}$,$hMLH1^{-}$); HCT116 $p53^{-/-}$ ($p53^{-/-}$,$hMLH1^{-}$).

7.2.2 Induction of apoptosis occurs mainly in $p53^{-/-}$ cells

To investigate if the strong sensitivity of the $p53^{-/-}$ cell line observed in MTT assay was due to apoptosis induction, different apoptotic assays were carried out after CPT-11 treatment.

The analysis of cell survival by trypan blue exclusion over several days after treatment showed that there is a concentration- (**Fig. 26A**) and time-dependent (**Fig. 26C**) cell death, the extent of which was different in the three cell lines. Six days after the start of treatment the death of $p53^{+/+}$,$hMLH1^{+}$ cells was about 10%, that in case of $p53^{+/+}$,$hMLH1^{-}$ cells reached a maximum of 40%, whereas it was 75% in the case of $p53^{-/-}$ cells (**Fig. 26C**). The Cell Death Detection ELISA (**Fig. 26B, D**), reflecting the enrichment of fragmented DNA, indicated that the observed cell death is due to prolonged apoptosis. Indeed, the cleavage of PARP reached in the $p53^{-/-}$ cell line 58% at 6 days after initiation of treatment (**Fig. 26E**). In contrast, the $p53^{+/+}$,$hMLH1^{+}$ cell line showed very little apoptosis and in the $p53^{+/+}$,$hMLH1^{-}$ cells the level of apoptosis was moderate in both latter assays (**Fig. 26D, E**).

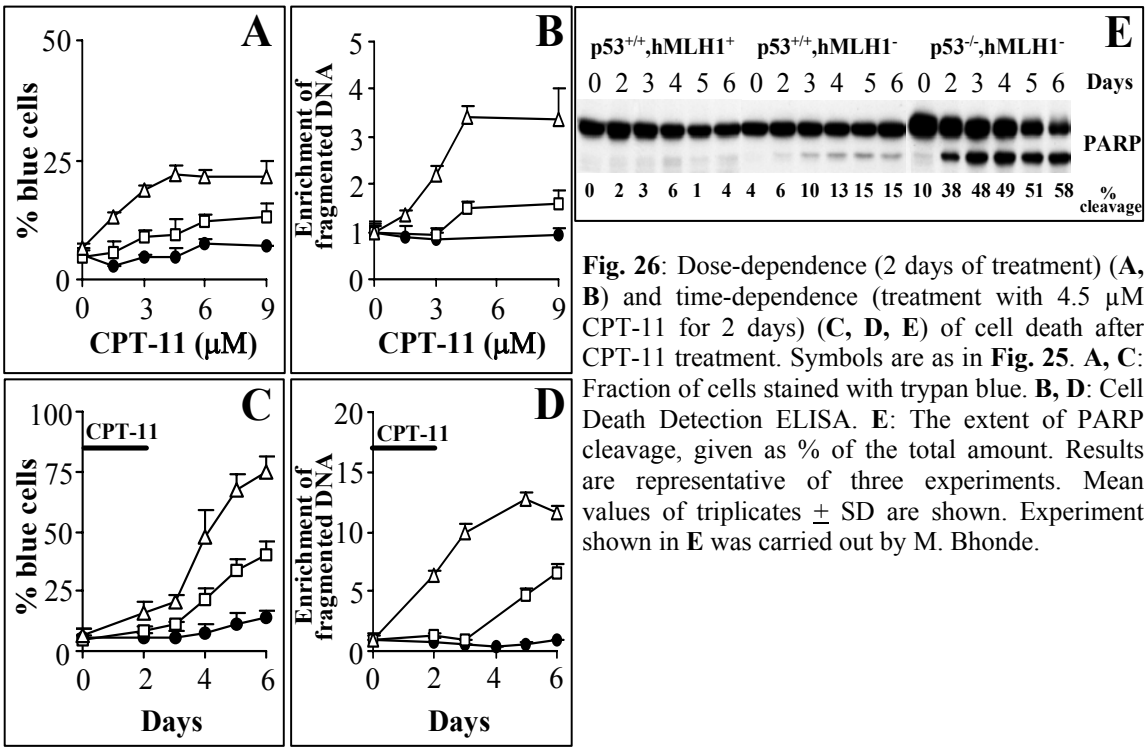

Fig. 26: Dose-dependence (2 days of treatment) (**A, B**) and time-dependence (treatment with 4.5 μM CPT-11 for 2 days) (**C, D, E**) of cell death after CPT-11 treatment. Symbols are as in **Fig. 25**. **A, C**: Fraction of cells stained with trypan blue. **B, D**: Cell Death Detection ELISA. **E**: The extent of PARP cleavage, given as % of the total amount. Results are representative of three experiments. Mean values of triplicates ± SD are shown. Experiment shown in **E** was carried out by M. Bhonde.

These results showed that the reaction to CPT-11 is different in the three cell lines and that it is affected by the p53- as well as by the hMLH1- status: $p53^{-/-}$,$hMLH1^{-}$ cells were undergoing a massive apoptosis, $p53^{+/+}$,$hMLH1^{-}$ underwent a moderate apoptotic process, while $p53^{+/+}$,$hMLH1^{+}$ cells were not undergoing apoptosis after CPT-11 treatment.

7.2.3 p53 protein is necessary for the induction, but not for the maintenance, of CPT-11-induced G2/M-phase arrest

Of particular interest was the high death rate of the $p53^{-/-}$ cells indicating that this process is p53-protein-independent. We further investigated, therefore, the effects of CPT-11 on the cell cycle.

Treatment with different concentrations of CPT-11 (1.5 μM, 4.5 μM and 12 μM) for 2 days induced in all three cell lines a G2/M-phase arrest of different duration (**Fig. 27A, B, C**). At 1.5 μM CPT-11, G2/M-phase arrest was barely detectable (**Fig. 27A**). At 4.5 μM CPT-11, the arrest was maintained in the $p53^{+/+}$,$hMLH1^{+}$ cell line for at least

twelve days. A slow release from the arrest in the $p53^{+/+}$,$hMLH1^{-}$ cell line occurred between 6 and 9 days from the start of treatment, indicating that the status of the hMLH1 molecule might indirectly or directly affect the maintenance of the G2/M-phase arrest. In the $p53^{-/-}$ cell line, by contrast, the G2/M-phase arrest was terminated already within 4 days from the start of treatment (**Fig. 27B**). This effect was particularly evident at 12 μM CPT-11 (**Fig. 27C**); at this concentration, the three cell lines were arrested in G2/M-phase to 90% after 2 days of treatment. The G2/M-phase arrest was released after 3 days from the start of treatment in the $p53^{-/-}$ cells, while $p53^{+/+}$ cells remained arrested in G2/M-phase for at least 4 days. The comparison of **Fig. 27 A, B** and **C** shows that while CPT-11-induced G2/M-phase arrest was prolonged and maintained in the two $p53^{+/+}$ cell lines, it was terminated already 3-4 days after start of treatment in $p53^{-/-}$ cells. The termination of the G2/M-phase arrest was accompanied in the $p53^{-/-}$ cells by a high percentage of apoptotic cells, visible in FACS as the subG1 peak. After treatment with 4.5 μM CPT-11, cells with subG1 DNA content reached 40% in the $p53^{-/-}$,$hMLH1^{-}$ cells after 6 days from the start while there were only about 10% in the $p53^{+/+}$,$hMLH1^{+}$ cells and about 20% in the $p53^{+/+}$,$hMLH1^{-}$ cells (**Fig. 27D**). These results corresponded to the previous data obtained in Cell Death Detection ELISA, PARP immunoblot and trypan blue staining (**Fig. 26**). Furthermore, the percentage of octaploid cells (DNA content = 8N) was different: while it was 10-15% in the $p53^{+/+}$ cells, it was less than 2% in the $p53^{-/-}$ cell line (**Fig. 27E, F**).

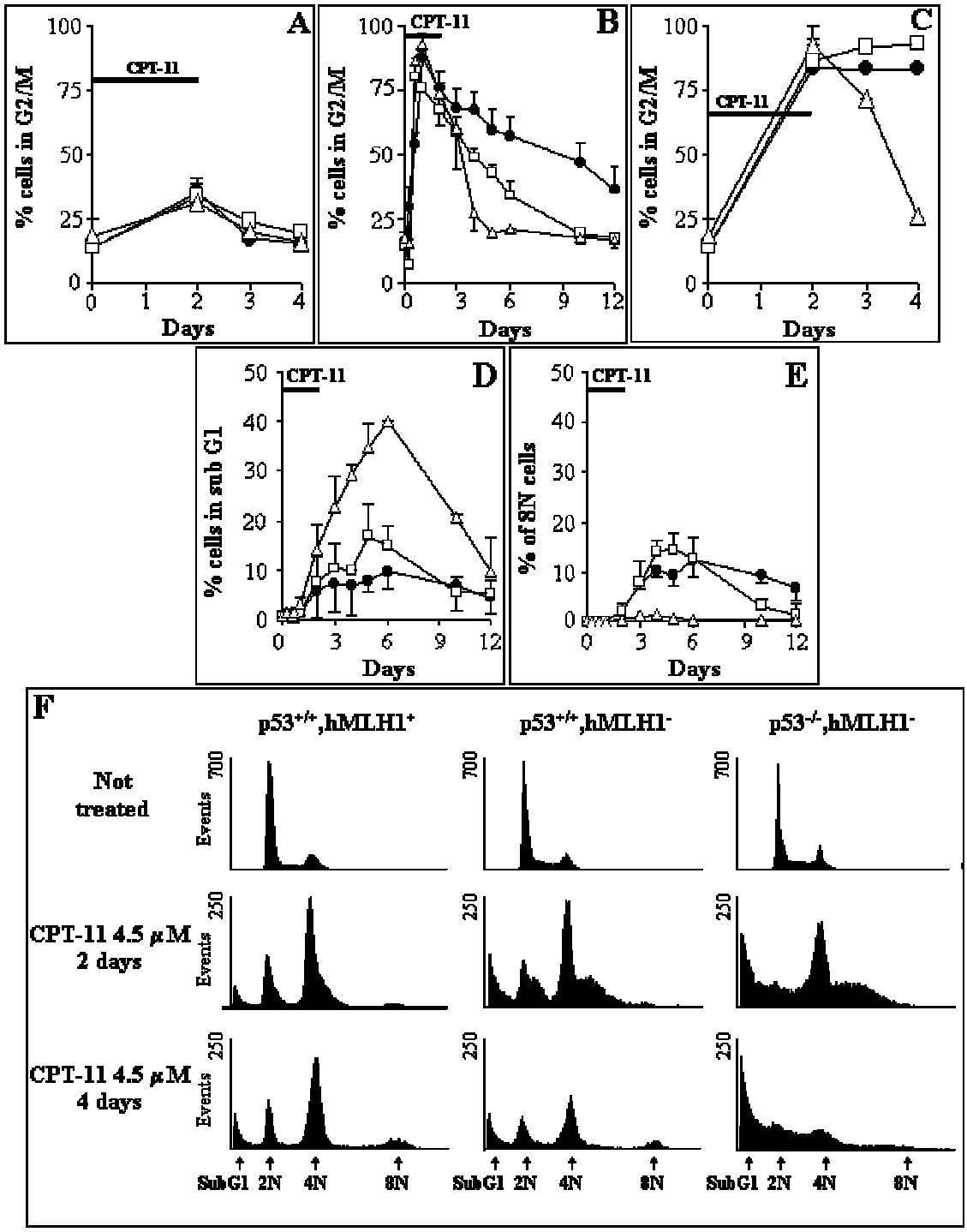

Fig. 27: CPT-11 induces a concentration- and time-dependent G2/M-phase arrest (**A**: 1.5 µM CPT-11 for 2 days; **B**: 4.5 µM CPT-11 for 2 days; **C**: 12 µM CPT-11 for 2 days), *p53* gene loss or hMLH1 defect affects **B, C**: The duration of G2/M-phase arrest, **D**: The extent of apoptosis determined as the subG1 fraction of cells, **E**: The formation of octaploid cells. **F**: Representative FACS diagrams for each non-treated cell line, *versus* treated for 2 days with 4.5 µM CPT-11 and assayed either immediately after termination of treatment (2 days) or 2 days after termination of treatment (4 days). Symbols are as in **Fig. 25**. Mean values of two to five experiments ± SD are shown.

The data obtained in FACS were corroborated by the evaluation of DAPI staining, performed on seeded cells at different time points after treatment. In the $p53^{+/+}$ cell lines the >4N cells emerged during the whole period of cell growth and were visible even after 14 days as large, sometimes solitary nuclei (**Fig. 28B, D**). The presence of the solitary nuclei suggested that some cells, arrested at the beginning of treatment, survived but did not form colonies. This was most pronounced in the $p53^{+/+}$,$hMLH1^{+}$ cell line, which also showed the longest maintenance of the G2/M-phase arrest. In contrast, $p53^{-/-}$ cells showed no solitary nuclei after 14 days, but formed colonies (**Fig. 28F**) comparable to the non-treated sample (**Fig. 28E**).

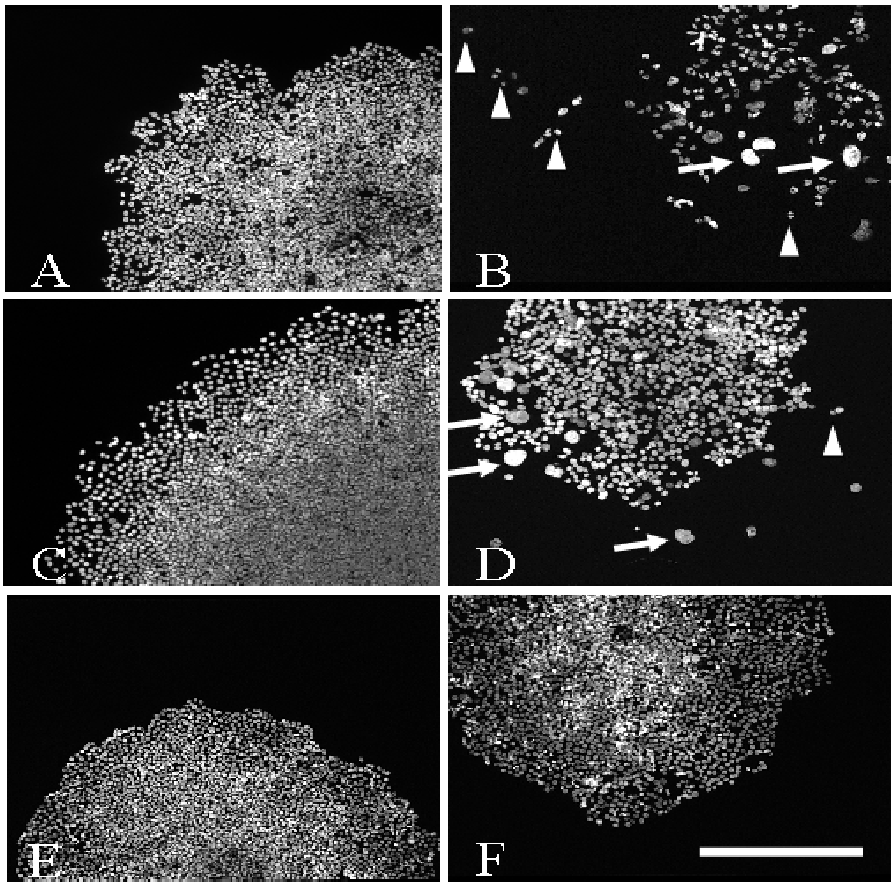

Fig. 28: DAPI staining of non-treated colonies of $p53^{+/+}$,$hMLH1^{+}$ (**A**), $p53^{+/+}$,$hMLH1^{-}$ (**C**) and $p53^{-/-}$,$hMLH1^{-}$ cells (**E**) or colonies of the same cell lines grown for 6 days after CPT-11 treatment for 2 days (4.5 μM) (**B, D, F**). Arrowheads: Single arrested cells not forming colonies. Arrows: Polyploid cells. In the $p53^{-/-}$ cell line polyploid cells undergoing apoptosis were seen 5 days after start of treatment (not shown). Results are representative of three independent experiments. Bar: 500 μm.

Thus, the detailed long-term analysis of cell cycle arrest and cell death showed that CPT-11 induced excessive apoptosis in $p53^{-/-}$ cells but a long-term cell cycle arrest with no or little apoptosis in $p53^{+/+}$ cells.

7.2.4 CPT-11-induced G2/M-phase arrest prevents apoptosis in $p53^{+/+}$ cells

To test if the apoptosis observed in $p53^{-/-}$ cells is the consequence of the lack of G2/M-phase arrest maintenance or rather a parallel independent process, the effects of artificial abrogation or of artificial induction of the G2/M-phase arrest were followed. The partial abrogation of the G2/M-phase arrest with caffeine lead to a 10-20% increase of the percentage of cells with a subG1 DNA content in the $p53^{+/+}$ cell lines (**Fig. 29**). The abrogation of the arrest and the extent of apoptosis were similar in $hMLH1^{+}$ (**Fig. 29A**) or in $hMLH1^{-}$ cells (**Fig. 29B**). Conversely, the artificial arrest in G2/M-phase of $p53^{-/-}$ cells with nocodazole partly inhibited the CPT-11-induced PARP cleavage (**Fig. 29C**).

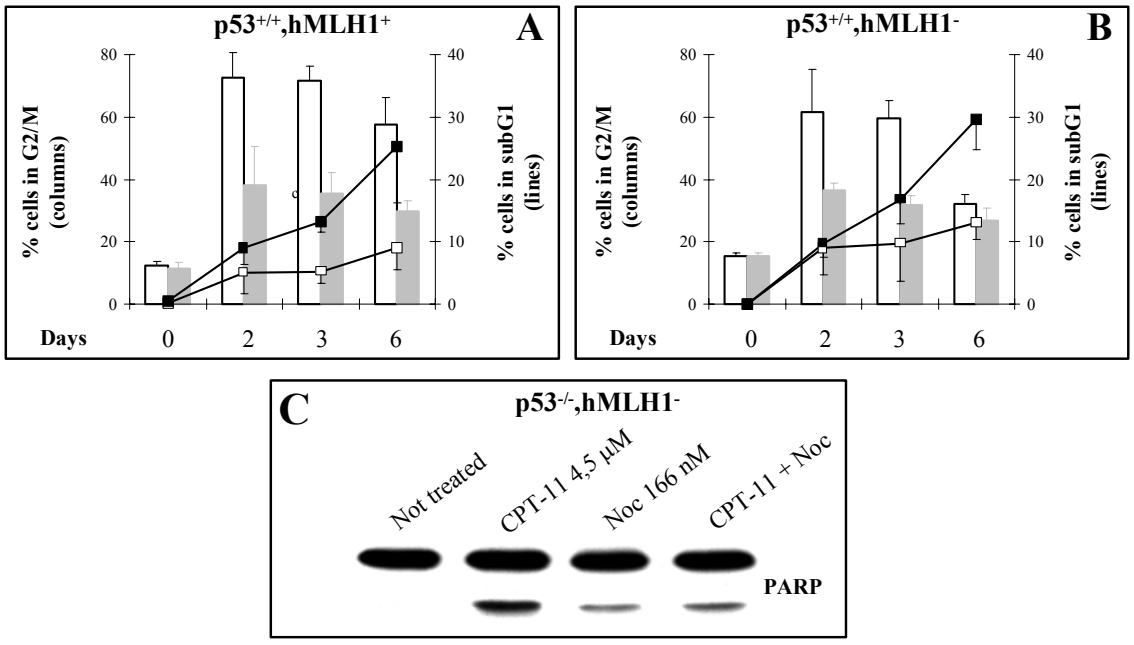

Fig. 29: A, B: Caffeine partially abrogates G2/M-phase arrest and induces increase in apoptosis in $p53^{+/+}$,$hMLH1^{+}$ cells (**A**) or in $p53^{+/+}$,$hMLH1^{-}$ cell (**B**). Columns: G2/M-phase arrest after addition of CPT-11 (4.5 µM, 2 days) alone ☐ or CPT-11 + caffeine (1.5 mM, 2 days) ▒ . Lines: subG1 fraction in the presence of CPT-11 alone —□— or CPT-11 + caffeine —■— . Treatment with caffeine alone showed no cells in subG1. Mean values of three independent experiments ± SD are shown. **C**: Nocodazole treatment (2 days, 166 nM) partially inhibits in $p53^{-/-}$ cells PARP cleavage induced by CPT-11. M. Bhonde performed the experiment shown in **C**.

Collectively, these data indicate that the CPT-11-induced apoptosis in $p53^{-/-}$ cells is due to lack of a prolonged G2/M-phase arrest, and that the functional G2/M-phase arrest contributes to prevention of apoptosis.

7.2.5 Induction of G2/M-phase arrest is associated with phosphorylation of cdc2 at Tyr-15

To clarify the mechanism triggered by CPT-11 and leading to the G2/M-phase arrest, the phosphorylation status of cdc2 protein was investigated. The phosphorylation of cdc2 at Tyr-15, which is known to inhibit the kinase activity, rapidly increased in all three cell lines and reached a maximum at 1-2 days after start of treatment; then it quickly returned to the basal level (**Fig. 30**). Since the expression of cdc2 protein did not change in this time interval (**Fig. 30**), these changes reflected the specific phosphorylation of cdc2 protein.

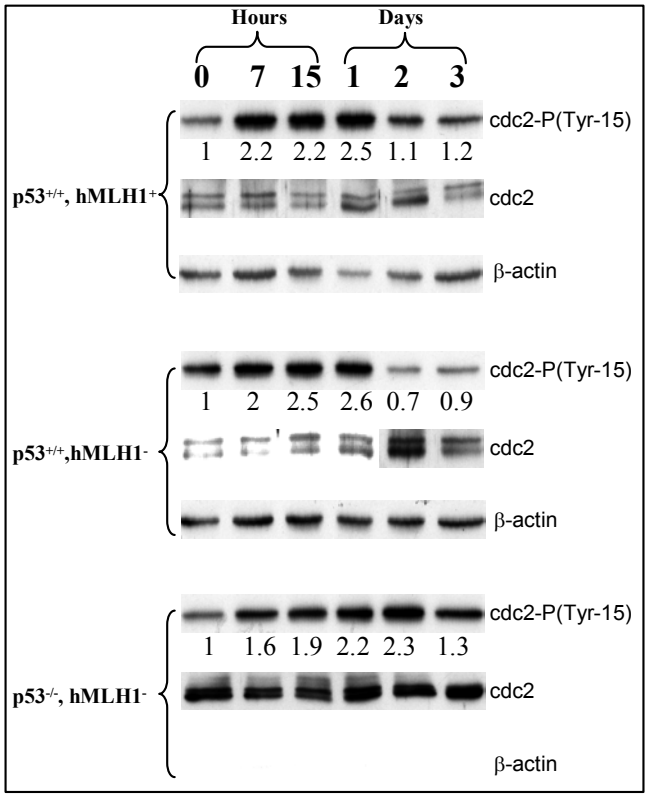

Fig. 30: Time course of expression of phosphorylated cdc2, cdc2-P(Tyr-15), and total cdc2 protein at different time points from the start of treatment. Western blot of lysates, detected on different membranes with antibody against phosphorylated cdc2 at Tyr-15 or with antibody against cdc2 protein. 20 µg of lysates were applied to each lane. ß-actin band, detected for control of the loaded protein amount, was the same in all lanes. Numbers denote relative band intensity in relation to the intensity in the non-treated sample. Results are representative of three independent experiments.

These data indicated that the increase of cdc2 phosphorylation after CPT-11 treatment was common to all three cell lines and independent from p53- and hMLH1-status. They were interpreted to indicate that the initial inhibitory phosphorylation of cdc2 is responsible for the triggering of the G2/M-phase arrest in the three cell lines.

7.2.6 Maintenance of G2/M-phase arrest is associated with binding of $p21^{CIP1}$ protein to cdc2/cyclin B1 complex and inhibition of cdc2 kinase activity

To clarify the mechanism leading to the maintenance of CPT-11-induced G2/M-phase arrest in the $p53^{+/+}$ cells, further investigations were performed by Western blot and immunoprecipitation.

Treatment of $p53^{+/+}$ cells triggered a massive overexpression of p53 and $p21^{CIP1}$ proteins (**Fig. 31A**), which reached a maximum at 2 days and was maintained for several days at this level. In the $p53^{-/-}$ cell line, a faint expression of $p21^{CIP1}$ was detectable at days 3-5 after start of treatment (**Fig. 31A**); this could indicate a p53-independent mechanism of $p21^{CIP1}$ induction after CPT-11 treatment.

The $p53^{-/-}$ cell line showed a high cdc2 kinase activity at five days after the start of CPT-11 treatment (**Fig. 31B**), at the time point where the G2/M-phase arrest is already terminated and apoptosis is high (compare **Fig. 27B**). At this time point both $p53^{+/+}$ cell lines were still arrested and the kinase activity, as measured by phosphorylation of histone H1, was low (**Fig. 31B**). Thus the overexpression of $p21^{CIP1}$ protein in the $p53^{+/+}$ cell lines was concomitant with the inhibition of cdc2 kinase activity.

As expected, in the immunoprecipitates of the cdc2/cyclin B1 complexes from the $p53^{+/+}$ cell lines also $p21^{CIP1}$ protein could be detected, indicating that five days after start of treatment the inhibition of cdc2 kinase is due to the binding of $p21^{CIP1}$ to cdc2 (**Fig. 31B**). The scanning of the autoradiogram indicated that the binding of $p21^{CIP1}$ was concomitant with a decrease of the cdc2 kinase activity to about 30% (**Fig. 31B**).

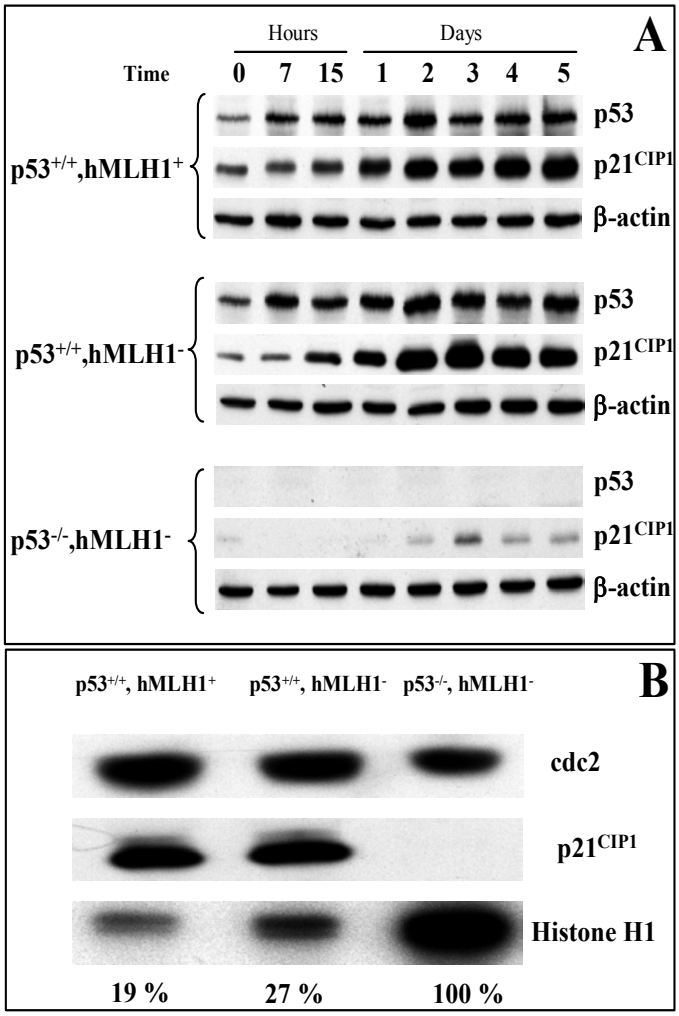

Fig. 31: **A**: Alterations of expression of p53- and of $p21^{CIP1}$- proteins after treatment with 4.5 µM CPT-11 for 2 days. ß-actin band, detected for control of the loaded protein amount, was the same in all lanes. **B**: Precipitations were carried out with the anti-cyclin B1 antibody from the three cell lines five days after start of treatment and were analysed for the presence of cdc2 and $p21^{CIP1}$ proteins by Western blot. Kinase activity in the precipitated cdc2/cyclin B1 protein complex was measured as histone H1 phosphorylation and visualized by autoradiography. Equal amounts of cdc2 protein were present in each precipitate, $p21^{CIP1}$ protein was detectable in the precipitates from $p53^{+/+}$ cells but not from the $p53^{-/-}$ cell line. M. Bhonde carried out experiments shown in **B**.

Collectively, these data are compatible with the hypothesis that while the G2/M-phase arrest was triggered in the three cell lines by a brief phosphorylation of cdc2 at Tyr-15, the long-lasting maintenance of the arrest was due to the cdc2 kinase inhibition through $p21^{CIP1}$ binding and was operative only in $p53^{+/+}$ cells.

7.2.7 CPT-11-induced apoptosis in $p53^{-/-}$ cells is correlated with inhibition of expression of the anti-apoptotic protein Bcl-X_L

In order to elucidate the mechanism of the observed cell death in $p53^{-/-}$ cells after CPT-11 treatment, the expression of several molecules known to be involved in apoptosis induction was analysed.

The levels of Bax and Bcl-2 expression were not significantly changed during 6 days from the start of treatment (**Fig. 32,** upper panel). By contrast, the expression of Bcl-X_L

was decreased by more than 50% only in $p53^{-/-}$ cells after treatment with CPT-11 (**Fig. 32**, upper panel). Thus the ratio of Bax/Bcl-X_L was not or only moderately changed in $p53^{+/+}$ cells but it was increased in the $p53^{-/-}$ cell line, suggesting that the amount of free Bax was increased (**Fig. 32**, lower panel).

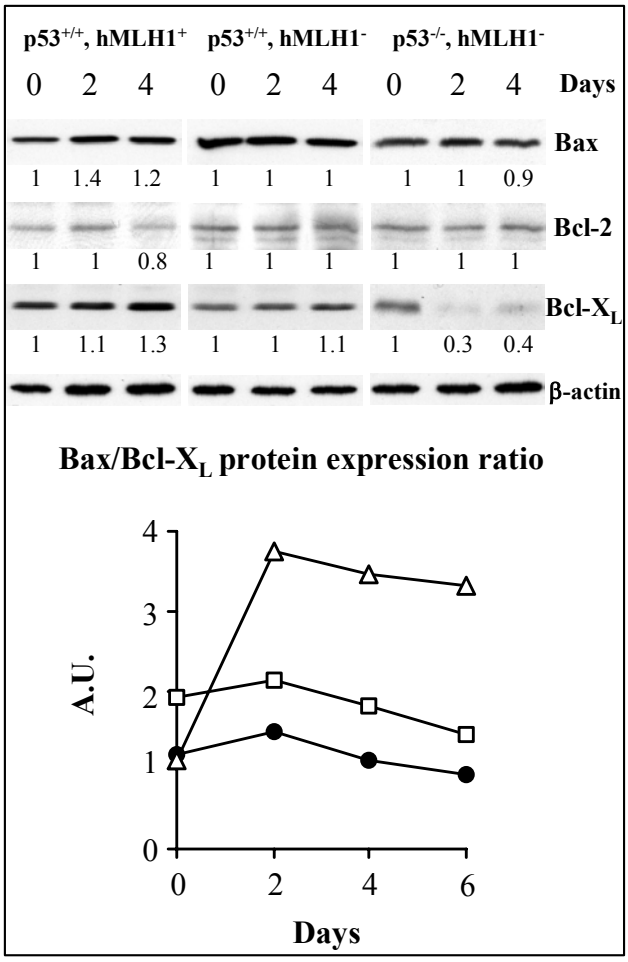

Fig. 32: Ratio of the amounts of Bax/Bcl-X_L in the three cell lines is increasing only in $p53^{-/-}$ cells. **Upper panel**: Alterations of expression of Bax, Bcl-2, and Bcl-X_L after treatment of the three cell lines with CPT-11 (4.5 μM for 2 days). Numbers denote relative band intensity in relation to the intensity in the non-treated samples. 20 μg of protein were loaded to each lane. **Lower panel**: Bax and Bcl-X_L proteins were detected on the same membrane. The 6-days time point was compared to the control value on another membrane. A.U.: Arbitrary units. Results are representative of three experiments. Symbols are as in **Fig. 25**.

These data support the hypothesis that Bcl-X_L might be one of the effector molecules in $p53^{-/-}$ cells after CPT-11 treatment; its downregulation may lead to liberation of Bax protein and consequently to a p53-independent apoptosis induction.

In conclusion, we could show in the isogenic cell system, that the presence of p53 or hMLH1 proteins affects the cellular responses to CPT-11. $p53^{+/+}$ cells were arrested in G2/M-phase, and this was protecting them from apoptosis. $p53^{-/-}$ cells underwent apoptosis after treatment with CPT-11. The extent of apoptosis correlated in this cell line with an increase of levels of free Bax protein. Moreover, cells with a functional hMLH1 molecule underwent a stronger G2/M-phase arrest and less apoptosis than hMLH1-deficient cells.